Cell

GPR120 Is an Omega-3 Fatty Acid Receptor Mediating Potent Anti-inflammatory and Insulin-Sensitizing Effects

Da Young Oh,[1,4] Saswata Talukdar,[1,4] Eun Ju Bae,[1] Takeshi Imamura,[2] Hidetaka Morinaga,[1] WuQiang Fan,[1] Pingping Li,[1] Wendell J. Lu,[1] Steven M. Watkins,[3] and Jerrold M. Olefsky[1,*]
[1]Department of Medicine, Division of Endocrinology and Metabolism, University of California, San Diego, La Jolla, CA 92093, USA
[2]Division of Pharmacology, Shiga University of Medical Science, Tsukinowa, Seta, Otsu-city, Shiga, 520-2192 Japan
[3]Tethys Bioscience, 3410 Industrial Boulevard, Suite 103, West Sacramento, CA 95691, USA
[4]These authors contributed equally to this work
*Correspondence: jolefsky@ucsd.edu
DOI 10.1016/j.cell.2010.07.041

SUMMARY

Omega-3 fatty acids (ω-3 FAs), DHA and EPA, exert anti-inflammatory effects, but the mechanisms are poorly understood. Here, we show that the G protein-coupled receptor 120 (GPR120) functions as an ω-3 FA receptor/sensor. Stimulation of GPR120 with ω-3 FAs or a chemical agonist causes broad anti-inflammatory effects in monocytic RAW 264.7 cells and in primary intraperitoneal macrophages. All of these effects are abrogated by GPR120 knockdown. Since chronic macrophage-mediated tissue inflammation is a key mechanism for insulin resistance in obesity, we fed obese WT and GPR120 knockout mice a high-fat diet with or without ω-3 FA supplementation. The ω-3 FA treatment inhibited inflammation and enhanced systemic insulin sensitivity in WT mice, but was without effect in GPR120 knockout mice. In conclusion, GPR120 is a functional ω-3 FA receptor/sensor and mediates potent insulin sensitizing and antidiabetic effects in vivo by repressing macrophage-induced tissue inflammation.

INTRODUCTION

Chronic activation of inflammatory pathways plays an important role in the pathogenesis of insulin resistance and the macrophage/adipocyte nexus provides a key mechanism underlying the common disease states of decreased insulin sensitivity (Schenk et al., 2008). This involves migration of monocytes/macrophages to adipose tissue (including intramuscular fat depots) and liver with subsequent activation of macrophage proinflammatory pathways and cytokine secretion. Through paracrine effects, these events promote inflammation and decreased insulin sensitivity in nearby insulin target cells (Shoelson et al., 2007; Schenk et al., 2008). In these studies, we explore the interlocking biology between proinflammatory and anti-inflammatory molecules within the specialized population of proinflammatory tissue macrophages.

G protein-coupled receptors (GPCRs) are important signaling molecules for many aspects of cellular function. They are members of a large family that share common structural motifs such as seven transmembrane helices and the ability to activate heterotrimeric G proteins, such as Gαs, Gαi, and Gαq. Ligands bind specifically to GPCRs to stimulate and induce a variety of cellular responses via several second messenger pathways; e.g., modulation of cAMP production, the phospholipase C pathway, ion channels, and mitogen-activated protein kinases (Ulloa-Aguirre et al., 1999; Gether, 2000; Schulte and Fredholm, 2003. Recently, several groups reported that five orphan receptors, GPR40, GPR41, GPR43, GPR84, and GPR120, can be activated by free fatty acids (FFAs). Short-chain fatty acids (FAs) are specific agonists for GPR41 and GPR43 (Tazoe et al., 2008) and medium-chain FAs for GPR84 (Wang et al., 2006a). Long-chain FAs can activate GPR40 (Itoh et al., 2003) and GPR120 (Hirasawa et al., 2005). Hirasawa et al. showed that the stimulation of GPR120 by FFAs resulted in elevation of $[Ca^{2+}]_i$ and activation of the ERK cascade which suggests interactions with the Gαq family of G proteins. However, other physiological functions of GPR120 remain to be explored. In the current study, we found that GPR120 was highly expressed in adipose tissue, and proinflammatory macrophages. The high expression level of GPR120 in mature adipocytes and macrophages indicates that GPR120 might play an important role in these cell types. We stimulated GPR120 with a synthetic agonist (GW9508) and omega-3 fatty acids (ω-3 FAs) and examined whether activation of GPR120 affected LPS- and TNF-α-induced inflammatory signaling responses. While SFAs are proinflammatory and unsaturated FAs are generally neutral, we found that ω-3 FAs (docosahexaenoic acid (C22:6n3, DHA) and eicosapentaenoic acid (C20:5n3, EPA)), the major ingredients in fish oil, exert potent anti-inflammatory effects through GPR120.

β-arrestins can serve as scaffold or adaptor proteins for a wide range of GPCRs, as well as a selected group of other receptor subtypes (Miller and Lefkowitz, 2001). After ligand binding, β-arrestins can associate with the cytoplasmic domains of

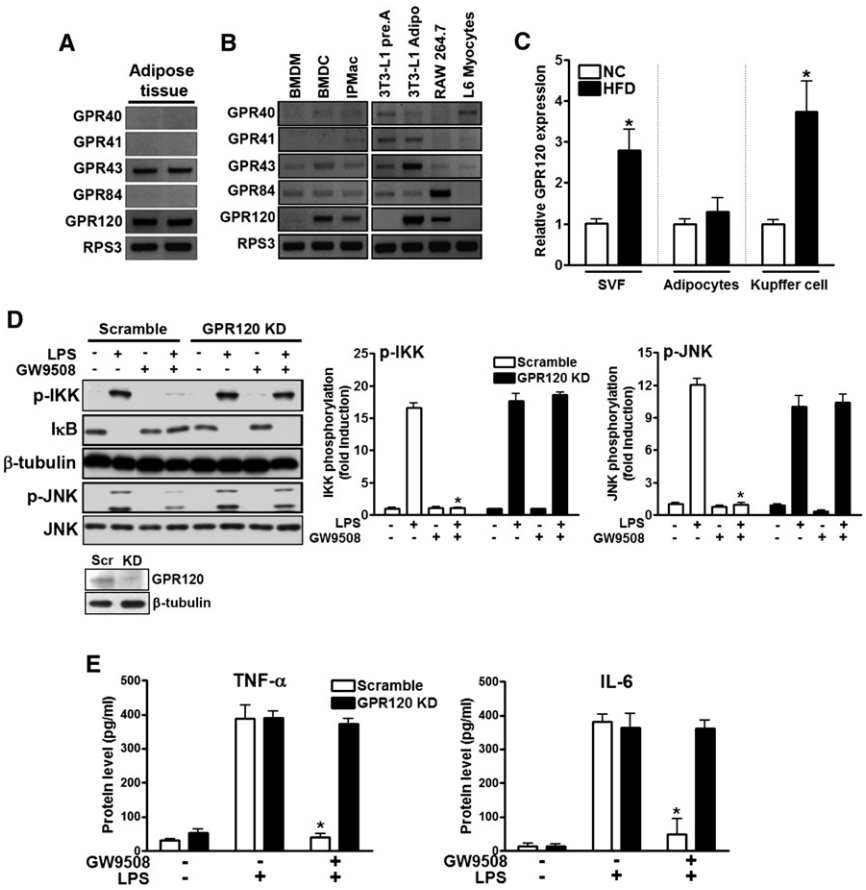

Figure 1. Expression Level of GPR120 and GPR120-Mediated Anti-inflammatory Response in RAW 264.7 Cells

(A and B) (A) The mRNA expression pattern of various lipid sensing GPCRs is shown in adipose tissue, (B) CD11c$^+$ bone marrow-derived dendritic cells (BMDCs), bone marrow-derived macrophages (BMDMs), IPMacs, 3T3-L1 preadipocytes, differentiated 3T3-L1 adipocytes, RAW 264.7 cells, and L6 myocytes. Ribosomal protein S3 (RPS3) was used as internal control.

(C) Expression of GPR120 in SVF, adipocytes and hepatic Kupffer cells from chow (NC)- or HFD-fed mice was examined by q-PCR. Data are expressed as the mean ± SEM of at least three independent experiments in triplicate. *$p < 0.05$ versus NC.

(D) RAW 264.7 cells, transfected with scrambled (Scr) or GPR120 #2 siRNA (GPR120 KD), were treated with 100 μM of GW9508 for 1 hr prior to LPS (100 ng/ml) treatment for 10 min and then subjected to western blotting. Left panel is a representative image from three independent experiments, and the scanned bar graph (right panel) shows fold induction over basal conditions. Knockdown efficiency of GPR120 siRNA is shown in Figure S1.

(E) Cytokine secretion level was measured in RAW 264.7 cells by ELISA. Data are expressed as the mean ± SEM of three independent experiments. *$p < 0.05$ versus LPS treatment in scrambled siRNA transfected cells. See also Figures S1 and S2.

GPCRs and couple the receptor to specific downstream signaling pathways, as well as mediate receptor endocytosis (Luttrell and Lefkowitz, 2002). Here we find that β-arrestin2 associates with ligand-stimulated GPR120 and participates in downstream signaling mechanisms.

Since chronic inflammation is a mechanistic feature of obesity-related insulin resistance, we postulated that the anti-inflammatory effect of GPR120 stimulation could promote insulin sensitization. In the present study, we elucidate the role of GPR120 activation in integrating anti-inflammatory and insulin sensitizing effects in vitro and in vivo.

RESULTS

GPR120 Expression

Fatty acids (FAs) can function as endogenous ligands modulating inflammatory responses, but not all FAs work in the same way. In general, saturated FAs (SFAs) are proinflammatory, unsaturated FAs are weakly proinflammatory or neutral, and ω3-FAs can be anti-inflammatory (Lee et al., 2003; Calder, 2005; Solinas et al., 2007). Because of the importance of inflammation in a number of chronic human diseases including insulin resistance, obesity, and type 2 diabetes mellitus, we surveyed the family of FA sensing GPCRs (GPR40, 41, 43, 84, and 120). Based on its tissue expression pattern, GPR120 emerged as a receptor of particular interest. As seen in Figure 1, GPR120 is the only lipid sensing GPCR which is highly expressed in adipose tissue, proinflammatory CD11c$^+$ macrophages (BMDCs), mature adipocytes, and monocytic RAW 264.7 cells (Figure 1A and 1B). GPR120 is induced in the stromal vascular fraction (SVF) of adipose tissue (which contains the macrophages), as well as in hepatic Kupffer cells, during high-fat diet (HFD) feeding in mice (Figure 1C). GPR120 is also expressed in enteroendocrine L cells with negligible expression in muscle (Figure S4C available online), hepatocytes or other cell types (Hirasawa et al., 2005; Gotoh et al., 2007).

Ligand-Stimulated GPR120 Exerts Anti-inflammatory Effects

It has been previously reported that GPR120 signals via a Gαq/11-coupled pathway and can respond to long chain FAs (Hirasawa et al., 2005). To pursue the biology of GPR120, a tool compound was needed, and, some years ago, Glaxo published GW9508 as a GPR40 selective agonist. However, this compound was not specific and also stimulated GPR120 (Briscoe et al., 2006). Since macrophages and adipocytes do not express GPR40 (this was confirmed by repeated q-PCR and RT-PCR measures, Figure S1A), GW9508 is a functional GPR120 specific compound in these cell types. Using this approach, we found that GW9508 treatment broadly and markedly repressed the ability of the TLR4 ligand LPS to stimulate inflammatory responses in RAW 264.7 cells (Figure 1D and E).

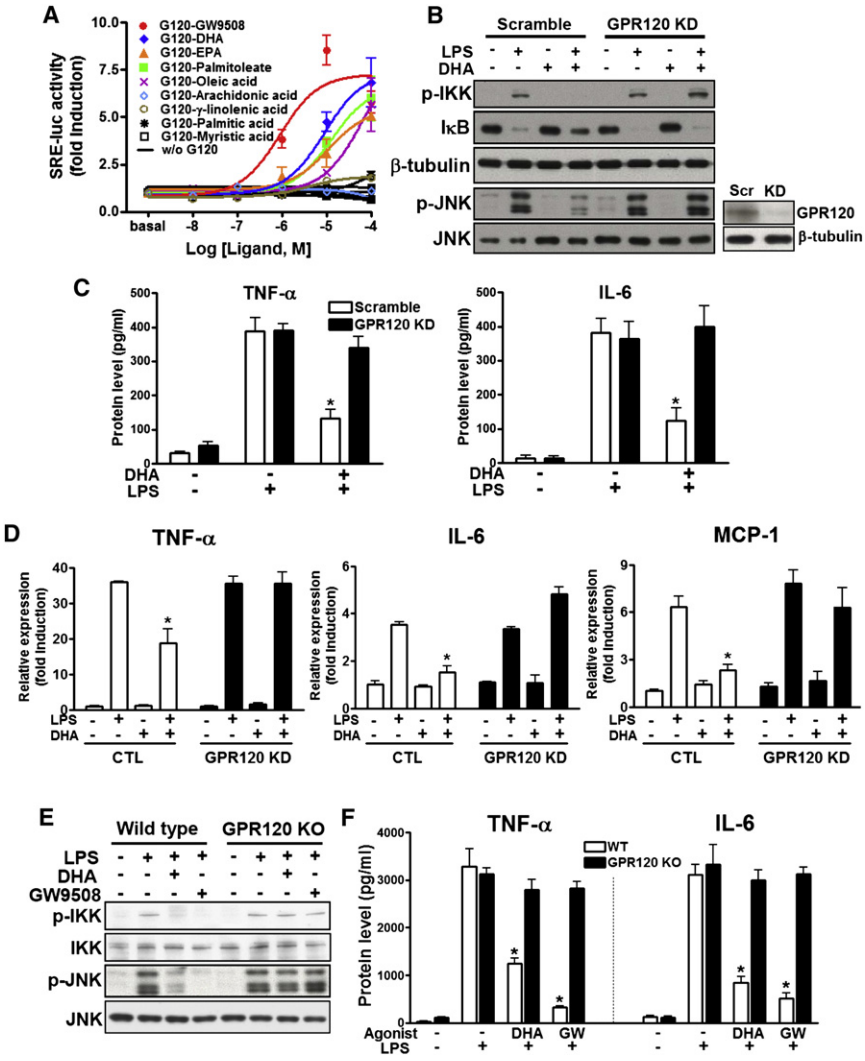

Figure 2. Omega-3 FA Stimulates GPR120 and Mediates Anti-inflammatory Effects

(A–D) GPR120-mediated SRE-luc activity after treatment with various FAs. Results are fold activities over basal. Each data point represents mean ± SEM of three independent experiments performed in triplicate. Black lines indicate SRE-luc activities without GPR120 transfection or with non-stimulating FAs. DHA inhibits LPS-induced inflammatory signaling (B), cytokine secretion (C), and inflammatory gene mRNA expression level (D) in RAW 264.7 cells, but not in GPR120 knockdown cells.

(E and F) GPR120 stimulation inhibits LPS-induced inflammatory response in WT primary macrophage. Data are expressed as the mean ± SEM of three independent experiments. *$p < 0.05$ versus LPS treatment in scrambled siRNA transfected cells or WT IPMacs. See also Figure S2.

Thus, GW9508 inhibited LPS stimulated phosphorylation of IKKβ and JNK, prevented IκB degradation, and inhibited TNF-α and IL-6 secretion. All of these effects of GW9508 were completely abrogated by siRNA mediated knockdown of GPR120 (Figures 1D and 1E and Figure S1F).

Based on these remarkable anti-inflammatory effects of GPR120 stimulation, we established a cell based reporter system by transfecting HEK293 cells with constructs for GPR120 along with a serum response element-luciferase promoter/reporter (SRE-luc). Since GPR120 is a Gαq/11-coupled receptor, it stimulates both PKC and MAP kinase, and both of these biologic effects are detected by the SRE-driven reporter system (Oh et al., 2005). The reporter cells were treated with various FAs and the synthetic GW9508 ligand. We found that GW9508, the ω-3 FAs (DHA and EPA) and palmitoleate (C16:1n7), all activated the SRE-luc reporter with an EC_{50} of 1-10 μM (Figure 2A), while SFAs were without effect. GW9508 and DHA were used at 100 μM in all subsequent studies to achieve maximal action. The ω-3 FAs (DHA and α-linolenic acid), and SFA (palmitic acid (C16:0)) activated ERK phosphorylation in RAW 264.7 cells, but only DHA- and α-linolenic acid-mediated ERK phosphorylation were abolished by GPR120 knockdown (Figure S2A). These results indicate that ω-3 FAs, but not SFAs, specifically activated ERK via GPR120.

The activation of GPR120 by ω-3 FAs, as well as its expression in adipocytes and macrophages, led us to study whether DHA, a representative ω-3 FA, can modulate inflammation through GPR120 in these cells. To examine this, we pretreated RAW 264.7 cells and 3T3-L1 adipocytes with GW9508 or DHA for 1 hr, followed by LPS (TLR4), TNF-α, TLR2, or TLR3 stimulation, respectively. We found that GW9508 and, more importantly, DHA, strongly inhibited LPS-induced phosphorylation of JNK and IKKβ, IκB degradation, cytokine secretion and inflammatory gene expression level in RAW 264.7 cells (Figures 2B–2D) as well as TNF-α, TLR2 and TLR3-induced JNK and IKKβ phosphorylation in 3T3-L1 adipocytes (Figure S2B) or RAW 264.7 cells (Figure S2C). All of the effects of GW9508 and DHA were completely prevented by GPR120 knockdown, demonstrating that these anti-inflammatory effects were specifically exerted through GPR120 (Figure 1, Figure 2, Figure S1, and Figure S2). Similar results were seen in primary wild-type (WT) intraperitoneal macrophages (IPMacs) and GPR120 knockout (KO) IPMacs (Figures 2E and 2F). These data argue that GPR120 is an ω-3 FA receptor or sensor, and provide a molecular mechanism for the anti-inflammatory effects of this class of FAs.

Role of β-arrestin2 in GPR120 Signaling

Given these potent cell selective anti-inflammatory effects, it was of interest to understand the specific mechanisms whereby signals from GPR120 inhibit inflammatory pathways. To further assess this, we used RNA interference to examine

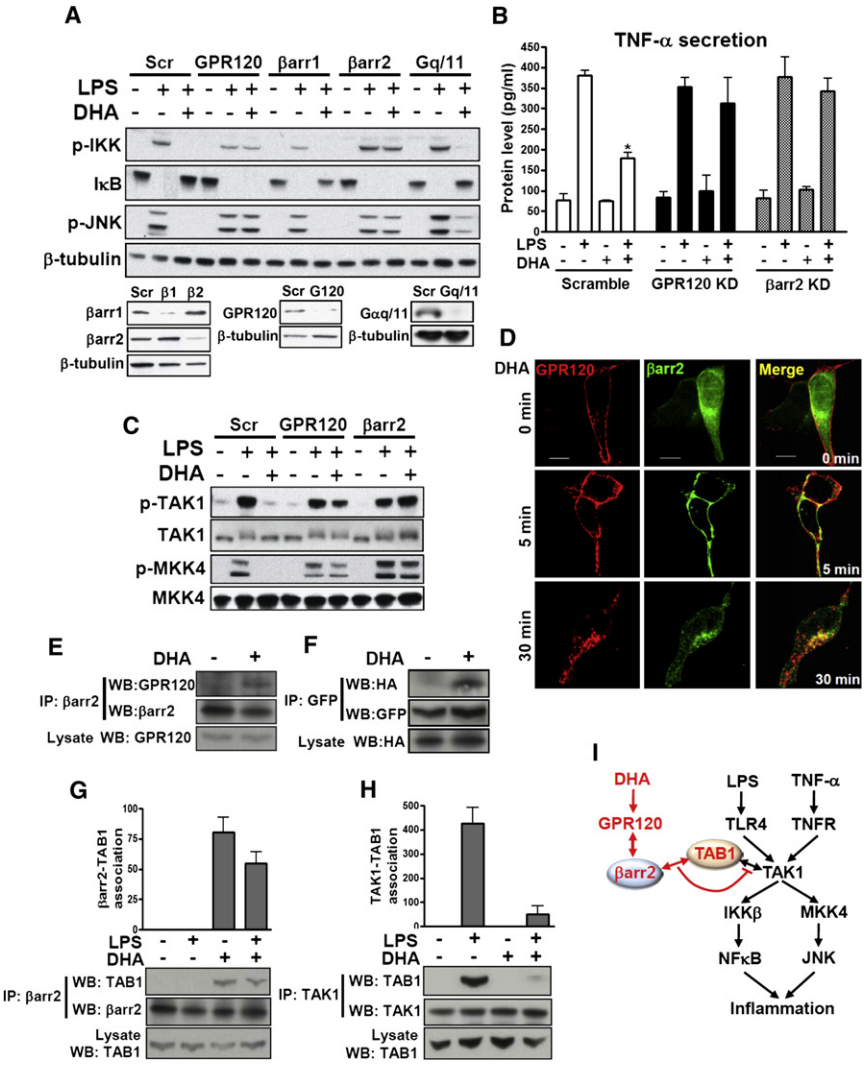

Figure 3. GPR120 Internalization with β-arrestin2 Mediates Anti-inflammatory Effects

(A) RAW 264.7 cells were transfected with siRNA as indicated and stimulated with or without 100 μM of DHA 1 hr prior to LPS (100 ng/ml) treatment for 10 min and then subjected to western blotting.

(B) TNF-α secretion was measured in RAW 264.7 cell cultured media with or without RNA interference as indicated.

(C) Phosphorylation of TAK1 and MKK4 in RAW 264.7 cells with or without siRNA transfection as indicated.

(D) HEK293 cells were cotransfected with HA-GPR120 and β-arrestin2·GFP to analyze GPR120 internalization after DHA stimulation for the indicated times. GPR120 (red) and β-arrestin2 (green) were localized by confocal microscopy.

(E–H) (E) Coimmunoprecipitation between GPR120 and β-arrestin2 with DHA stimulation for 30 min in RAW 264.7 cells and, (F) HEK293 cells (HA-GPR120 and β-arrestin2·GFP), respectively. Lysate indicates 1/10 input in each experiment. Interaction between TAB1 and β-arrestin2 (G) and interaction between TAB1 and TAK1 (H) were detected by coimmunoprecipitation and the scanned bar graph quantitates the association in RAW 264.7 cells.

(I) Schematic diagram of the β-arrestin2 and GPR120-mediated anti-inflammatory mechanism. Red colored letters and arrows indicate the DHA-mediated anti-inflammatory effect, and black colored letters and arrows indicate the LPS- and TNF-α-induced inflammatory pathway. See also Figure S2.

molecules involved in generation of GPR120 signals. As seen in Figures 3A and 3B, LPS signaling was not affected by β-arrestin1, -2, or Gαq/11 knockdown. However, with β-arrestin2 knockdown, DHA-mediated anti-inflammatory signaling was extinguished, while β-arrestin1 and Gαq/11 knockdown were without effect (Figure 3A).

Figure 3A and Figure S2 show that GPR120 stimulation inhibits both TLR4- and TNF-α mediated inflammatory responses. Since the TNF-α and TLR signaling cascades converge downstream of GPR120 activation, these results indicate that the site of GPR120-induced inhibition is either at, or upstream, of JNK/IKKβ. LPS activates inflammation through the TLR4 pathway by engaging the serine kinase IRAK, leading to phosphorylation of transforming growth factor-β activated kinase 1 (TAK1) which is upstream of MKK4/JNK and IKKβ (Kawai and Akira, 2006, Figure 3I). TNF-α and TLR2/3 also leads to stimulation of TAK1, resulting in activation of IKKβ and JNK (Takaesu et al., 2003). Consequently, we determined whether DHA stimulation of GPR120 inhibited TAK1 and MKK4. As seen in Figure 3C, DHA treatment abrogated LPS-induced TAK1 and MKK4 phosphorylation in a GPR120 and β-arrestin2-dependent manner. Since TLR2/3/4 and TNF-α signaling were inhibited by GPR120 activation, these results indicate that DHA signaling intersects at TAK1 and inhibits all upstream input activating signals via a GPR120/β-arrestin2 interaction (Figure 3I).

After ligand stimulation, β-arrestin2 can translocate to a number of GPCRs where it mediates receptor internalization and signaling (Barak et al., 1997). We transfected HEK293 cells with β-arrestin2·GFP to visualize intracellular trafficking of β-arrestin2 following activation of GPR120 (Figure 3D). In the basal state, GPR120 was localized to the plasma membrane as assessed by immunostaining (red fluorescence, Figure 3D), while β-arrestin2 exhibited a diffuse, largely cytoplasmic staining pattern (green, Figure 3D). Following DHA treatment for 5 min, β-arrestin2·GFP translocated from the cytosol to the plasma membrane and can be seen colocalized with GPR120 (merged, right fields). After 30 min of DHA treatment, much of the GPR120 is internalized, as visualized by punctate intracellular staining (lower left panel), and β-arrestin2·GFP is now colocalized with the intracellular GPR120 (lower right panel, Figure 3D). DHA-stimulated binding of β-arrestin2 to activated GPR120 was also detected by coimmunoprecipitation (Figure 3E and F).

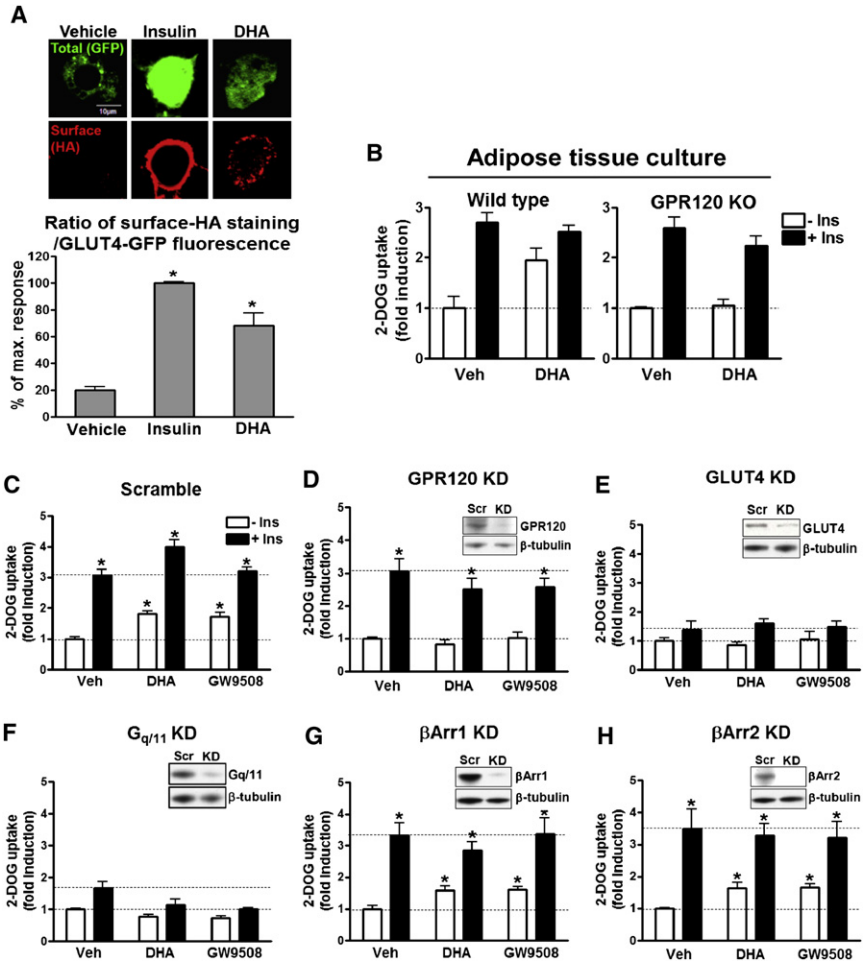

Figure 4. GPR120 Activation Enhances GLUT4 Translocation and Glucose Uptake

(A) 3T3-L1 adipocytes were transfected with a dually tagged HA-GLUT4-GFP construct. Total GLUT4 expression was determined by GFP fluorescence, and GLUT4 translocation to the cell surface after 100 ng/ml insulin or 100 μM DHA stimulation for 30 min was determined by indirect immunofluorescence of the HA-conjugated with Alexa 594 in fixed cells. Translocation following insulin stimulation was expressed as a percentage of the maximum response. The bar graph represents the mean ± SEM data from four independent experiments. *$p < 0.05$ versus vehicle treatment. (B) Glucose uptake was measured in WT and GPR120 KO mouse primary adipose tissue and in (C–H) 3T3-L1 adipocytes ± siRNA with the indicated treatment. Data are expressed as mean ± SEM of three independent experiments in triplicate. *$p < 0.05$ versus basal activity. The indicated siRNA knockdown efficiency was validated by western blotting. See also Figure S3.

LPS or TNF-α signaling activate TAK1 by causing the association of TAK1 binding protein 1 (TAB1) with TAK1. Figure 3H shows that LPS stimulation of RAW 264.7 cells causes TAB1/TAK1 association. DHA treatment leads to the association of β-arrestin2 with TAB1 (Figure 3G) and largely blocks TAK1/TAB1 association (Figure 3H). To further examine the interaction site of β-arrestin2 and GPR120 or TAB1, we pursued coimmunoprecipitation with a series of β-arrestin2 truncation/deletion mutants (Figure S2D). Full-length β-arrestin2 was able to bind to GPR120 and TAB1 only in the presence of DHA, clearly showing the DHA dependency of this interaction. Interestingly, only the full-length β-arrestin2 coprecipitated with GPR120 and TAB1, while a series of deletion/truncation β-arrestin2 mutants did not, indicating that the interactions are dependent on the complete tertiary structure of β-arrestin2 (Figure S2D; Luttrell et al., 1999). Taken together, these results suggest that GPR120 activation leads to association of β-arrestin2 with the receptor and that this complex subsequently internalizes, whereupon β-arrestin2 can bind to TAB1. The data further suggest that association of β-arrestin2 with TAB1 blocks TAB1/TAK1 binding, resulting in inhibition of TAK1 phosphorylation and activation (Figure 3I).

GPR120 Activation Enhances Glucose Uptake in 3T3-L1 Adipocytes

Since our data show that GPR120 is expressed in mature adipocytes and signals through Gαq/11 in these cells, we assessed the effects of GPR120 stimulation on insulin sensitivity in primary adipose tissue cultures and in 3T3-L1 adipocytes. Primary adipose tissue explants and 3T3-L1 adipocytes were pretreated for 30 min with GW9508 or DHA, followed by measurement of basal and insulin stimulated GLUT4 translocation (Figure 4A) and 2-deoxyglucose (2-DOG) transport (Figures 4B–4H). Ligand-stimulation of GPR120 led to an increase in glucose transport and translocation of GLUT4 to the plasma membrane in adipocytes, but was without effect in muscle cells (Figure S4D) which don't express GPR120 (Figure 1B and Figure S4C). This stimulatory effect of DHA and GW9508 was blocked when GPR120 or Gαq/11 was depleted by siRNA knockdown (Figure 4D and Figure 4F). GLUT4 knockdown also blocked the effects of DHA and GW9508, while the effects of insulin were decreased by ~90% (Figure 4E). This, along with the GLUT4 translocation data provided in Figure 4A, indicates that the stimulatory effects of GPR120 are indeed working through GLUT4. Further assessment of this pathway showed that DHA had a modest effect to stimulate phosphorylation of Akt, but that this was abrogated with GPR120 knockdown (Figure S3A). The effects of DHA to stimulate Akt were blocked by inhibiting PI3 kinase with LY294002 (Figure S3B). Finally, DHA did not stimulate IRS-1 phosphorylation (Figure S3C), indicating that its glucose transport stimulatory effects were downstream of IRS-1. Knockdown of Gαq/11 also completely blocked the effects of DHA to stimulate glucose transport (Figure 4F), while β-arrestin1 or -2 knockdown was without effect (Figures 4G

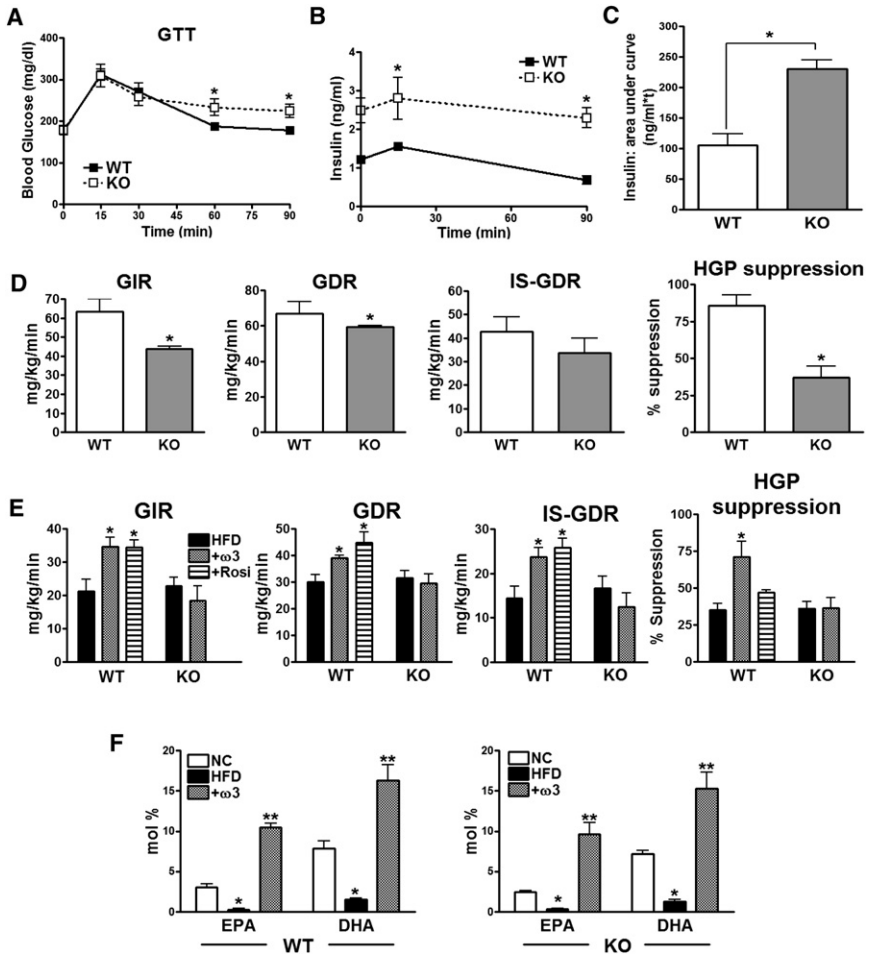

Figure 5. In Vivo Metabolic Studies in GPR120 KO Mice

(A) GTT in NC-fed WT and GPR120 KO mice. n = 7 per group.

(B and C) Insulin concentration was measured at the indicated time points and (C) area-under-curve analysis of the insulin data shows a significant difference between WT and GPR120 KO mice on NC.

(D) Hyperinsulinemic/euglycemic clamp studies in chow-fed WT and GPR120 KO mice.

(E) Clamp studies in HFD, ω-3 FA supplemented (+ω3), and Rosiglitazone treated HFD mice (+Rosi). n = 8 per group, *p < 0.05 compared to HFD-fed WT group.

(F) Mean ± SEM plasma concentration (mole (%)) of DHA and EPA for each diet in WT and GPR120 KO mice. n = 7 per each group. *p < 0.05, compared to NC, and **p < 0.05 compared to HFD. Data are represented as mean ± SEM. See also Figure S4, Figure S5, Figure S6, and Table S2.

and 4H). Interestingly, Gαq/11 knockdown not only inhibited DHA and GW9508 stimulated glucose transport, but it also attenuated insulin stimulatory effects, and the latter is fully consistent with previous publication (Imamura et al., 1999) showing the role of Gαq/11 in insulin signaling to glucose transport in adipocytes. This scheme is shown in Figure S3D.

In Vivo Metabolic Studies in GPR120 KO Mice

Since chronic tissue inflammation can cause insulin resistance, we hypothesized that deletion of GPR120 would enhance the proinflammatory tone, promoting glucose intolerance and decreased insulin sensitivity. To test this idea, GPR120 KO mice and WT littermates were evaluated on normal chow diet (NC). Body weights were similar in both groups, and as summarized in Figure 5, glucose tolerance tests (GTT) showed a mild degree of impairment in GPR120 KO animals compared to WTs (Figure 5A). More impressively, insulin secretion was more than 2-fold greater in the KO animals, and the combination of hyperinsulinemia and mild glucose intolerance indicates the presence of insulin resistance (Figures 5B and 5C). This was confirmed by performing hyperinsulinemic/euglycemic clamp studies in the chow fed WT and KO mice (Figure 5D). These studies revealed a 31% decrease in the glucose infusion rate (GIR) required to maintain euglycemia in the KO mice. Since 70%–80% of total body insulin stimulated glucose disposal is accounted for by skeletal muscle glucose uptake (Baron et al., 1988), the decreased insulin stimulated (IS)-glucose disposal rate (GDR) provides direct evidence for skeletal muscle insulin resistance in the KO mice. Likewise, the GPR120 KO mice exhibited a marked decrease in the ability of insulin to suppress hepatic glucose production (HGP), demonstrating the presence of hepatic insulin resistance. Thus, the decreased GIR was ~50% related to muscle and ~50% due to liver insulin resistance, respectively. Since the chow diet contains exogenous ω-3 FAs, we conclude that blunted ω-3 FA signaling in the KO mice, accounts for the decreased insulin sensitivity.

Since ω-3 FA administration can improve insulin sensitivity in rats (Buettner et al., 2006), we reasoned that ω-3 FA supplementation could alleviate HFD/obesity-induced insulin resistance in WT mice, but would be ineffective in GPR120 KOs. Accordingly, WT and GPR120 KO mice were placed on 60% HFD for 15 weeks. At this point, separate groups of 15 mice each, were treated for five additional weeks with 60% HFD or an isocaloric HFD diet containing 27% fish oil supplementation enriched in ω-3 FAs. This diet provided 50 and 100 mg of DHA and EPA, respectively, per mouse, per day. Figure 5E shows that administration of the ω-3 FA diet led to improved insulin sensitivity with increased glucose infusion rates, enhanced muscle insulin sensitivity (increased IS-GDR), greater hepatic insulin sensitivity (increased HGP suppression), and decreased hepatic steatosis (Figures S6A and S6B). Importantly, the ω-3 FA diet was completely without effect in the GPR120 KO mice. A separate group of WT mice were treated with the insulin sensitizing thiazolidinedione Rosiglitazone, and the effects of ω-3 FAs were equal to or greater (HGP suppression) than the effects of this clinically used insulin sensitizing drug.

In addition to improving hepatic insulin sensitivity, ω-3 FA treatment had a beneficial effect on hepatic lipid metabolism, causing decreased liver triglycerides, DAGs, along with reduced SFA and ω-6 FA content in the various lipid classes (Figures S6A–S6C and Table S2). The ω-3 FA supplementation was entirely without effect, or much less effective, at reducing hepatic lipid levels in the GPR120 KOs.

Interestingly, in the absence of ω-3 FA supplementation, GPR120 KO mice were just as susceptible to HFD-induced insulin resistance as were the WT mice. We hypothesize that this was because the 60% HFD is relatively deficient of exogenous ω-3 FAs, so that ligands for GPR120 were relatively absent in these animals. To assess this, we performed a lipomics analysis of the various fatty acid classes in the chow and HFD-fed WT and KO mice. As predicted, circulating concentrations of ω-3 FAs were much lower on HFD compared to chow diets, and the administration of the ω-3 FA supplement to the HFD led to a large increase in plasma ω-3 FA content in both genotypes (Figure 5F). This would account for the relative lack of effect of GPR120 KO on HFD alone, since ω-3 FA ligand stimulation is negligible, while the KO animals displayed an insulin resistant phenotype on chow diets when a moderate level of ω-3 FAs was provided. Importantly, the GPR120 KO mice are completely refractory to the insulin sensitizing effects of ω-3 FA administration on HFD.

To address the contribution of macrophages to the overall in vivo phenotype, we performed bone marrow transplantation (BMT) from GPR120 KOs into irradiated WT mice (adoptive transfer) to generate hematopoietic cell deletion of GPR120. The studies in the BMT WT and BMT GPR120 KO mice on chow diet revealed a highly significant 20%–30% decrease in GIR in the KOs, with a more dramatic impairment in the ability of insulin to suppress hepatic glucose production (Figure S4A). Thus, the studies in the BMT animals on the chow diet are comparable to the results (Figure 5D) observed in WT versus whole body GPR120 KOs on chow diet. When studied on the HFD ± ω-3 FA supplementation (Figure S4B), the ω-3 FA supplemented BMT GPR120 KO animals exhibited a 30% decrease in GIR compared to the ω-3 FA supplemented BMT WTs. This was explained by skeletal muscle insulin resistance (decreased ISGDR) and hepatic insulin resistance (decreased HGP suppression) in the GPR120 KOs compared to the WT BMT mice on the ω-3 FA supplemented HFD. These data are fully consistent with the results in the global KOs (Figure 5E) and reinforce the concept that the in vivo phenotype we observed can be largely traced to hematopoietic cells/macrophages.

Omega-3 FAs Reduce Inflammatory Macrophages in Adipose Tissue

We conducted histologic examination of adipose tissue macrophages (ATMs) from WT and GPR120 KO mice on HFD or the ω-3 FA enriched HFD by immunostaining for the M1 macrophage marker F4/80 and the M2 macrophage marker MGL1 (Lumeng et al., 2008) (Figure 6A). Consistent with previous studies (Weisberg et al., 2003; Xu et al., 2003; Nguyen et al., 2007), HFD induced a large increase in F4/80 positive ATMs, which form crown-like structures (CLS) around adipocytes in both WT and GPR120 KO mice. In contrast, MGL1 staining was minimal in both groups on HFD (Figure 6A). On the ω-3 FA diet, we observed a decrease in F4/80 staining, along with a marked increase in MGL1 positive cells in WT mice. Importantly, no change in F4/80 or MGL1 staining was noted in the GPR120 KO mice on the ω-3 FA diet. SVFs were prepared from adipose tissue and analyzed by flow cytometry to quantitate the total number of ATMs, as well as the content of $CD11b^+$ and $CD11c^+$ and negative macrophage subpopulations (Figure 6B). HFD led to a large but comparable increase in $CD11b^+$ and $CD11c^+$ ATM content in WT and GPR120 KO mice (Figure 6B, middle panel). Treatment with the ω-3 FA-enriched HFD caused a striking decrease in $CD11b^+$ and $CD11c^+$ ATMs in WT mice, but was without effect in the GPR120 KO group (Figure 6B, right panel). Thus, the FACS analysis was fully consistent with the histological results. Interestingly, $CD11c^+$ ATM content was also greater in the GPR120 KOs on the chow diet relative to WT consistent with the insulin resistance in the KO animals.

It seemed possible that the reduction in ATM content in WT animals on the ω-3 FA diet reflected decreased chemotaxis of macrophages. To test this hypothesis, we measured the migratory capacity of IPMacs from WT and GPR120 KO mice using an in vitro transwell chemotaxis assay. As seen in Figure 6C, macrophages from both groups readily migrated toward conditioned media (CM) harvested from 3T3-L1 adipocytes. Pretreatment of macrophages with DHA for 3 hr before exposure to CM led to an 80% inhibition of chemotactic capacity in WT macrophages, but had no significant effect on IPMacs obtained from the GPR120 KO mice. Similar experiments were performed using the specific chemokine, monocyte chemotactic protein-1 (MCP-1) as a chemoattractant, rather than CM, and these experiments yielded identical results (Figure 6D). These data indicate that ω-3 FAs cause decreased macrophage chemotaxis by acting through the GPR120 receptor, contributing to the differences in ATM content seen in Figures 6A and 6B.

Omega-3 FAs Decrease M1 Proinflammatory Gene and Increase M2 Anti-inflammatory Gene Expression in Adipose Tissue

As shown in Figure 7A, expression of M1 inflammatory genes such as IL-6, TNF-α, MCP-1, IL-1β, iNOS, and CD11c was increased by HFD compared to chow diet in both genotypes, and was reduced in the ω-3 FA treated WT mice, but not in the GPR120 KO mice. Even on chow diet, expression of several inflammatory genes was higher in GPR120 KOs compared to WT, consistent with the insulin resistance observed in the chow-fed KO mice. Expression of the M2 anti-inflammatory genes, arginase 1, IL-10, MGL1, Ym-1, Clec7a, and MMR was increased by ω-3 FAs in WT, but not in the GPR120 KO adipose tissue (Figure 7B). These results are consistent with Figure 6 and demonstrate that the dietary change from HFD to ω-3 FA supplemented HFD resulted in an overall decreased proinflammatory profile in adipose tissue from WT, but not in GPR120 KO mice. These changes in gene expression were predominantly manifested in the SVF, except for MCP-1 and IL-6, which are known to be readily expressed in adipocytes (Figure S7). Qualitatively similar results were seen in the liver (Figures S6D and S6E).

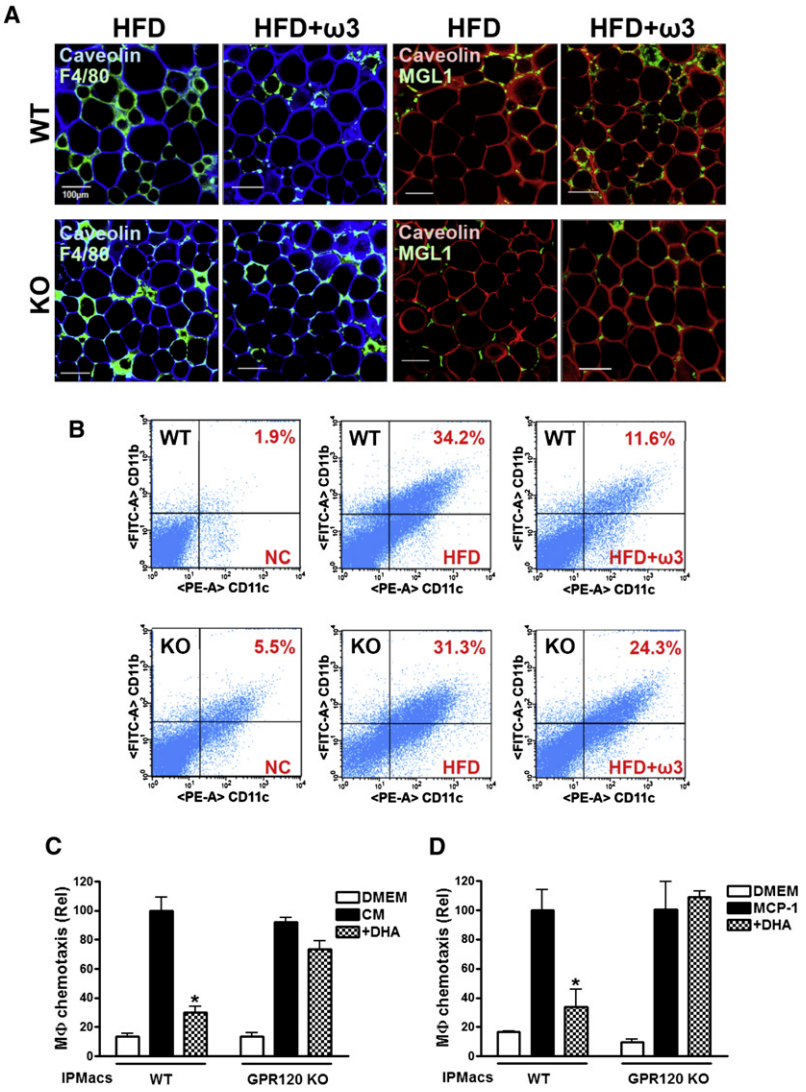

Figure 6. Omega-3 FA Enriched Diet Decreases Inflammatory Macrophage Infiltration in Adipose Tissue

(A) Confocal merged images from epididymal fat pads from HFD and ω-3 FA enriched HFD (HFD+ω3)-fed WT and GPR120 KO mice, costained with anti-F4/80 (green) and anti-Caveolin1 (blue) antibodies, left 4 panels, or anti-MGL1 (green) and anti-Caveolin1 (red) antibodies, right 4 panels. The image is representative of similar results from three to four independent experiments. Scale bar represents 100 μm.

(B) Dot plot representation of CD11b versus CD11c expression for FACS data obtained from adipose tissue SVF of NC, HFD or HFD+ω3-fed WT and GPR120 KO. Scattergram is representative from three independent mice from each group.

(C and D) Migratory capacity of IPMacs from WT and GPR120 KO mice as measured using an in vitro transwell chemotaxis assay as described under supplemental experimental procedures. Data are expressed as mean ± SEM of three independent experiments in triplicate. *, $p<0.05$ versus CM treatment.

DISCUSSION

In this report we show that GPR120 functions as an ω-3 FA receptor/sensor in proinflammatory macrophages and mature adipocytes. By signaling through GPR120, DHA and EPA (the major natural ω-3 FA constituents of fish oil), mediate potent anti-inflammatory effects to inhibit both TLR and TNF-α inflammatory signaling pathways. The mechanism of GPR120-mediated anti-inflammation involves inhibition of TAK1 through a β-arrestin2/TAB1 dependent effect. Since chronic tissue inflammation is an important mechanism causing insulin resistance (Xu et al., 2003; Shoelson et al., 2007; Schenk et al., 2008), the anti-inflammatory actions of ω-3 FAs exert potent insulin sensitizing effects. The in vivo anti-inflammatory and insulin sensitizing effects of ω-3 FAs are dependent on expression of GPR120, as demonstrated in studies of obese GPR120 KO animals and WT littermates. Thus, GPR120 is highly expressed in proinflammatory macrophages and functions as an ω-3 FA receptor, mediating the anti-inflammatory effects of this class of FAs to inhibit both the TLR2/3/4 and the TNF-α response pathways and cause systemic insulin sensitization.

GPR120 is a Gαq/11-coupled receptor, and since it is expressed in enteroendocrine L cells, past interest in this receptor has focused on its potential ability to stimulate L cell GLP-1 secretion. In the current study, we show that, in addition to L cells, GPR120 is highly expressed in proinflammatory, M1-like macrophages and mature adipocytes, with negligible expression in muscle, pancreatic β-cells, and hepatocytes (Gotoh et al., 2007). In the HFD/obese mouse model, GPR120 expression is highly induced in ATMs as well as resident liver macrophages (Kupffer cells). To explore the biology around GPR120, we established an artificial reporter cell assay and found that the ω-3 FAs, DHA, and EPA, are ligands for GPR120, and comparable to the effects of a non-selective GPR120 tool compound (GW9508), the ω-3 FAs exert potent anti-inflammatory effects in macrophages. Our results also revealed the molecular mechanisms underlying these anti-inflammatory effects. Thus, DHA stimulation of GPR120 inhibits both the TLR2/3/4 and TNF-α proinflammatory cascade. Since activation of IKKβ and JNK are common to TLR and TNF-α signaling, this indicates that the locus of GPR120 inhibition is at or proximal to these kinases. TAK1 activation stimulates both the IKKβ/NFκB and JNK/AP1 pathways, and the TLR and TNF-α signaling pathways converge at this step. Our data show that stimulation of GPR120 specifically inhibits TAK1 phosphorylation and activation providing a common mechanism for the inhibition of both TLR and TNF-α signaling.

Beta-arrestins can serve as important adaptor and scaffold molecules mediating the functions of a number of different GPCRs, as well as other receptor subtypes (Miller and Lefkowitz, 2001). The C-terminal region of GPR120 contains several

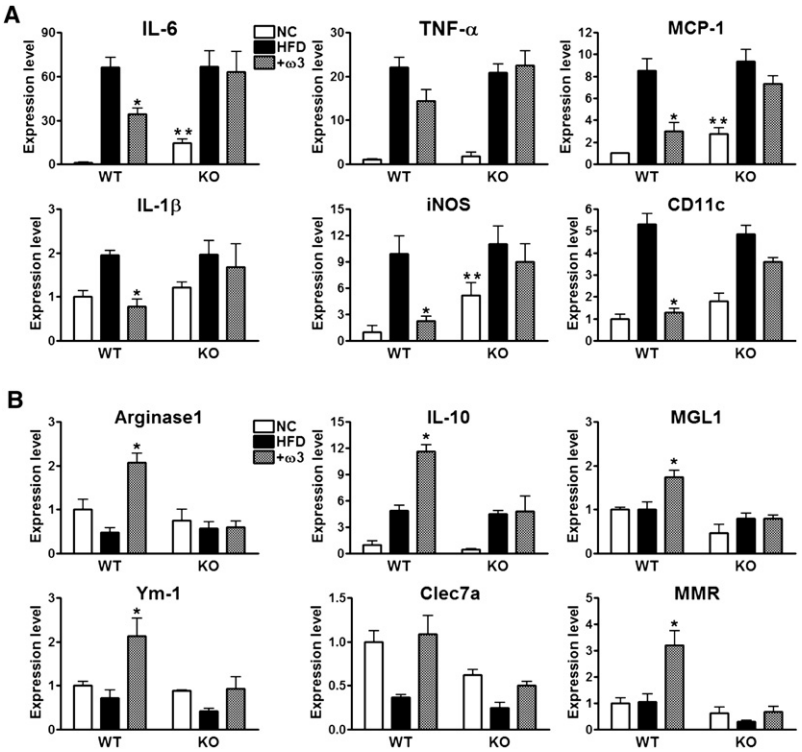

Figure 7. M1 and M2 Inflammatory Gene Expression Levels in Adipose Tissue from WT versus GPR120 KO Mice

Relative mRNA levels for M1 proinflammatory genes (A) and M2 anti-inflammatory genes (B) in NC, HFD, or HFD+ω3 (+ω3)-fed WT and GPR120 KO mice, as measured by q-PCR. Data are expressed as mean ± SEM of three independent experiments in triplicate. n=7 per group, *, $p<0.05$ compared to the HFD-fed WT group. **, $p<0.05$ compared to the WT versus GPR120 KO on NC. See also Figure S7. Primer sequences are shown in Table S1.

putative β-arrestin2 binding motifs [(S/T)X_{4-5}(S/T); Cen et al., 2001], but whether β-arrestins play any role in GPR120 function was unknown. Here we find that activation of GPR120 by DHA stimulation leads to association of the receptor with β-arrestin2, but not β-arrestin1, and that the anti-inflammatory effects of GPR120 are completely β-arrestin2 dependent. Functional immunocytochemical studies showed that DHA stimulation leads to recruitment of β-arrestin2 to the plasma membrane where it colocalizes with GPR120. This is followed by receptor and β-arrestin2 internalization, where the two are now colocalized in the cytoplasmic compartment. TAB1 is the activating protein for TAK1 and our results show that following DHA-stimulated internalization of the GPR120/β-arrestin2 complex, β-arrestin2 can now associate with TAB1, as measured in coimmunoprecipitation experiments; only full-length β-arrestin2 was capable of interacting with GPR120 and TAB1. This apparently blocks the association of TAB1 with TAK1, inhibiting TAK1 activation and downstream signaling to the IKKβ/NFκB and JNK/AP1 system. These results provide a mechanism for the β-arrestin2-mediated inhibition of TLR4, TNF-α, and TLR2/3 action. Other studies in the literature are consistent with these findings, since it has been shown that β-arrestin2 can inhibit NFκB signaling in other systems (Gao et al., 2004; Wang et al., 2006b). Furthermore, Lefkowitz' group has recently published an extensive proteomics analysis of β-arrestin2 interacting partners, and among the 266 proteins they identified, TAB1 was represented on the list (Xiao et al., 2007).

Interestingly, the anti-inflammatory effects mediated by GPR120 were entirely dependent on β-arrestin2, but independent of Gαq/11, despite the fact that GPR120 can be a Gαq/11-coupled receptor in other contexts. This provides further evidence demonstrating the concept that a single GPCR can independently signal through multiple pathways. In previous studies, we have demonstrated that Gαq/11 activation can lead to stimulation of GLUT4 translocation in adipocytes. Since GPR120 was expressed in mature adipocytes, but not preadipocytes, we explored the potential role of GPR120 in glucose transport control. Interestingly, we found that DHA stimulation of GPR120 in 3T3-L1 adipocytes increased GLUT4 translocation to the cell surface with a subsequent increase in glucose transport into the cells. RNA interference studies showed that the DHA effect on glucose uptake was GPR120, GLUT4, and Gαq/11 dependent, but independent of β-arrestin2. This effect was about 30%–50% as great as the effect of insulin and the actions of DHA on glucose uptake were additive to those of a submaximally stimulating concentration of insulin. From this, it is possible to propose that these insulinometic effects contribute to the overall insulin sensitizing actions of ω-3 FAs. However, muscle glucose uptake accounts for the great majority (70%–80%) of insulin stimulated glucose disposal. Furthermore, GPR120 is not expressed in muscle, and DHA did not stimulated glucose uptake in L6 myocytes (Figures S4C and S4D). In addition, acute administration of DHA had no stimulatory effects on IS-GDR (Figure S4E). This reports the conclusion that the in vivo stimulatory effects of DHA on GDR are related to anti-inflammation, and that the glucose transport stimulatory effects in adipocytes contribute little to the overall phenotype.

Since chronic, low grade tissue inflammation is an important cause of obesity-related insulin resistance, we reasoned that the anti-inflammatory effects of GPR120 stimulation should be coupled to insulin sensitizing actions in vivo. This idea was confirmed in studies of WT and GPR120 KO mice. On a chow diet, the lean GPR120 KO mice were glucose intolerant, hyperinsulinemic and displayed decreased skeletal muscle and hepatic insulin sensitivity, as measured during glucose clamp studies. They also displayed increased ATM content, relative to WT mice, and a 2- to 5-fold higher expression level of the M1 proinflammatory markers, MCP-1, iNOS, and IL-6 (Figure 7A). On HFD, GPR120 KO and WT mice became equally obese and insulin resistant. Importantly, ω-3 FA supplementation markedly increased insulin sensitivity in WT mice but was without effect in

the GPR120 KOs. Consistent with these results, ω-3 FA treatment led to a decrease in ATM accumulation with reduced adipose tissue markers of inflammation in WT, but not in KO mice. In addition to direct anti-inflammatory effects in macrophages, DHA treatment inhibited the ability of primary WT macrophages to migrate toward adipocyte CM. This could be due to DHA-induced decreased chemokine secretion or down-regulation of chemokine receptors, or both. In addition, it is possible that DHA, by signaling through GPR120, can mediate heterologous desensitization of other GPCR chemokine receptors. We also observed a concomitant increase in M2 markers, such as IL-10, arginase 1, MGL1, Ym-1, Clec7a, and MMR. This latter finding raises the possibility that ω-3 FAs can redirect ATMs from an M1 to an M2 polarization state. Taken together, these mechanisms account for the decreased inflammatory state. The in vivo anti-inflammatory actions of ω-3 FAs are consistent with the insulin sensitizing effects of these agents and are fully dependent on the presence of GPR120, indicating a causal relationship. Finally, the adoptive transfer studies showed that hematopoietic cell GPR120 deletion results in a comparable insulin resistant, ω-3 FA non-responsive phenotype as seen in the global GPR120 KOs, indicating that this phenotype can be traced back to inflammatory events in macrophages.

We also performed a detailed in vivo lipidomic analysis of FAs in the different lipid classes in the liver (Table S2). The results showed that HFD leads to an increase in total TAGs, DAGs, total SFAs, monounsaturated FAs and ω-6 FAs in WT mice, while all of these lipid changes are ameliorated with ω-3 FA treatment. In the GPR120 KO mice, all of these lipids are elevated on HFD to the same extent as in WT mice, but, ω-3 FA supplementation was either ineffective or much less effective. These results are consistent with the view that the reversal of steatosis/non-alcoholic fatty liver disease (NAFLD) by ω-3 FA treatment is mediated, in large part, by GPR120 and that the GPR120 KO mice are predisposed toward NAFLD even in the context of ω-3 FA supplementation.

Dietary DHA is rapidly esterified into chylomicrons during the process of gastrointestinal absorption, and is also packaged into VLDL triglycerides by the liver. DHA can also be esterified into phospholipids and cholesterol esters associated with circulating lipopoproteins and only a small proportion (~5%) of total plasma DHA is found in the FFA pool. Through the action of lipoprotein lipase bound to the luminal surface of endothelial cells, ω-3 FAs are cleaved from circulating triglycerides where they can act as ligands or be taken up by peripheral tissues (Polozova and Salem Jr., 2007). Recent studies have also indicated that metabolic products derived from ω-3 FAs, such as 17*S*-hydroxy-DHA, resolvins, and protectins may play a role in the long term resolution of inflammation and this might attenuate insulin resistance in the context of obesity (González-Périz et al., 2009). If this proves to be correct, then this could provide an additional mechanism for long term ω-3 FA-induced anti-inflammatory, insulin sensitizing effects. However, in the current studies, we found that these ω-3 FA derivatives were unable to stimulate GPR120 activation in our reporter cell assay (data not shown), indicating that GPR120 functions as a receptor for ω-3 FAs and not their biochemical products. Resolution of inflammation versus anti-inflammatory actions are distinct processes, and it is certainly possible that the products derived from ω-3 FA metabolism work on the former but not the latter.

In summary, we have found that GPR120 functions as an ω-3 FA receptor/sensor and mediates robust and broad anti-inflammatory effects, particularly in macrophages. After ligand stimulation, GPR120 couples to β-arrestin2 which is followed by receptor endocytosis and inhibition of TAB1-mediated activation of TAK1, providing a mechanism for inhibition of both the TLR and TNF-α proinflammatory signaling pathways. Since chronic tissue inflammation is linked to insulin resistance in obesity, we used GPR120 KO mice to demonstrate that ω-3 FAs cause GPR120-mediated anti-inflammatory and insulin sensitizing effects in vivo. Overall, these results strongly argue that anti-inflammatory effects can ameliorate insulin resistance in obesity. Taken together, GPR120 emerges as an important control point in the integration of anti-inflammatory and insulin sensitizing responses, which may prove useful in the future development of new therapeutic approaches for the treatment of insulin resistant diseases.

EXPERIMENTAL PROCEDURES

Chemicals and Reagents

GW9508 was purchased from Tocris bioscience (Ellisville, MO) and DHA was from Cayman chemical (Ann Arbor, MI). All other chemicals were purchased from Sigma unless mentioned otherwise.

Animal Care and Use

Male C57Bl/6 or GPR120 KO littermates were fed a normal chow (13.5% fat; LabDiet) or high-fat diet (60% fat; Research Diet) ad libitum for 15–20 weeks from 8 weeks of age. GPR120 KO mice and WT littermates were provided by Taconic Inc. (Hudson, NY). After 15 weeks on HFD, WT and GPR120 KO mice were switched to an isocaloric HFD-containing 27% menhaden fish oil replacement (wt/wt; menhaden fish oil: 16% EPA (C20:5n3), 9%, DHA (C22:6n3), Research Diet) (Jucker et al., 1999; Neschen et al., 2007) and fed for 5 weeks. Mice received fresh diet every 3rd day, and food consumption and body weight were monitored. Animals were housed in a specific pathogen-free facility and given free access to food and water. All procedures were approved by the University of California, San Diego animal care and use committee. In vivo metabolic studies were performed as described under supplemental experimental procedures.

Data Analysis

Densitometric quantification and normalization were performed using the ImageJ 1.42q software. The values presented are expressed as the means ± SEM. The statistical significance of the differences between various treatments was determined by one-way ANOVA with the Bonferroni correction using GraphPad Prism 4.0 (San Diego, CA). The $p < 0.05$ was considered significant.

SUPPLEMENTAL INFORMATION

Supplemental Information includes Extended Experimental Procedures, seven figures, and two tables and can be found with this article online at doi:10.1016/j.cell.2010.07.041.

ACKNOWLEDGMENTS

We thank Jachelle M. Ofrecio and Sarah Nalbandian for their help with animal maintenance and Elizabeth J. Hansen for editorial assistance. We are grateful to Dr. Robert Lefkowitz (Howard Hughes Medical Institute, Duke University) for the gift of FLAG-tagged serial mutant β-arrestin2 constructs and to Dr. Maziyar

Saberi at NGM Bio Inc. (San Francisco, CA) for GLP-1 measurements. We thank the Flow Cytometry Resource and Neal Sekiya for assistance with FACS analysis at the VA San Diego hospital, the UCSD Histology Core lab for technical help with processing liver specimens, and UCSD Microscope Resource for microscopy analysis. This study was funded in part by the National Institutes of Health grants NIDDK DK033651 (J.M.O.), DK063491 (J.M.O.), DK 074868 (J.M.O.), and the Eunice Kennedy Shriver NICHD/NIH through a cooperative agreement U54 HD 012303-25 as part of the specialized Cooperative Centers Program in Reproduction and Infertility Research.

Received: January 20, 2010
Revised: May 24, 2010
Accepted: July 19, 2010
Published: September 2, 2010

REFERENCES

Barak, L.S., Ferguson, S.S., Zhang, J., and Caron, M.G. (1997). A beta-arrestin/green fluorescent protein biosensor for detecting G protein-coupled receptor activation. J. Biol. Chem. *272*, 27497–27500.

Baron, A.D., Brechtel, G., Wallace, P., and Edelman, S.V. (1988). Rates and tissue sites of non-insulin- and insulin-mediated glucose uptake in humans. Am. J. Physiol. *255*, E769–E774.

Briscoe, C.P., Peat, A.J., McKeown, S.C., Corbett, D.F., Goetz, A.S., Littleton, T.R., McCoy, D.C., Kenakin, T.P., Andrews, J.L., Ammala, C., et al. (2006). Pharmacological regulation of insulin secretion in MIN6 cells through the fatty acid receptor GPR40: identification of agonist and antagonist small molecules. Br. J. Pharmacol. *148*, 619–628.

Buettner, R., Parhofer, K.G., Woenckhaus, M., Wrede, C.E., Kunz-Schughart, L.A., Scholmerich, J., and Bollheimer, L.C. (2006). Defining high-fat-diet rat models: metabolic and molecular effects of different fat types. J. Mol. Endocrinol. *36*, 485–501.

Calder, P.C. (2005). Polyunsaturated fatty acids and inflammation. Biochem. Soc. Trans. *33*, 423–427.

Cen, B., Xiong, Y., Ma, L., and Pei, G. (2001). Direct and differential interaction of beta-arrestins with the intracellular domains of different opioid receptors. Mol. Pharmacol. *59*, 758–764.

Gao, H., Sun, Y., Wu, Y., Luan, B., Wang, Y., Qu, B., and Pei, G. (2004). Identification of beta-arrestin2 as a G protein-coupled receptor-stimulated regulator of NF-kappaB pathways. Mol. Cell *14*, 303–317.

Gether, U. (2000). Uncovering molecular mechanisms involved in activation of G protein-coupled receptors. Endocr. Rev. *21*, 90–113.

González-Périz, A., Horrillo, R., Ferre, N., Gronert, K., Dong, B., Moran-Salvador, E., Titos, E., Martinez-Clemente, M., Lopez-Parra, M., Arroyo, V., and Claria, J. (2009). Obesity-induced insulin resistance and hepatic steatosis are alleviated by omega-3 fatty acids: a role for resolvins and protectins. FASEB J. *23*, 1946–1957.

Gotoh, C., Hong, Y.H., Iga, T., Hishikawa, D., Suzuki, Y., Song, S.H., Choi, K.C., Adachi, T., Hirasawa, A., Tsujimoto, G., et al. (2007). The regulation of adipogenesis through GPR120. Biochem. Biophys. Res. Commun. *354*, 591–597.

Hirasawa, A., Tsumaya, K., Awaji, T., Katsuma, S., Adachi, T., Yamada, M., Sugimoto, Y., Miyazaki, S., and Tsujimoto, G. (2005). Free fatty acids regulate gut incretin glucagon-like peptide-1 secretion through GPR120. Nat. Med. *11*, 90–94.

Imamura, T., Vollenweider, P., Egawa, K., Clodi, M., Ishibashi, K., Nakashima, N., Ugi, S., Adams, J.W., Brown, J.H., and Olefsky, J.M. (1999). G alpha-q/11 protein plays a key role in insulin-induced glucose transport in 3T3-L1 adipocytes. Mol. Cell. Biol. *19*, 6765–6774.

Itoh, Y., Kawamata, Y., Harada, M., Kobayashi, M., Fujii, R., Fukusumi, S., Ogi, K., Hosoya, M., Tanaka, Y., Uejima, H., et al. (2003). Free fatty acids regulate insulin secretion from pancreatic beta cells through GPR40. Nature *422*, 173–176.

Jucker, B.M., Cline, G.W., Barucci, N., and Shulman, G.I. (1999). Differential effects of safflower oil versus fish oil feeding on insulin-stimulated glycogen synthesis, glycolysis, and pyruvate dehydrogenase flux in skeletal muscle: a 13C nuclear magnetic resonance study. Diabetes *48*, 134–140.

Kawai, T., and Akira, S. (2006). TLR signaling. Cell Death Differ. *13*, 816–825.

Lee, J.Y., Plakidas, A., Lee, W.H., Heikkinen, A., Chanmugam, P., Bray, G., and Hwang, D.H. (2003). Differential modulation of Toll-like receptors by fatty acids: preferential inhibition by n-3 polyunsaturated fatty acids. J. Lipid Res. *44*, 479–486.

Lumeng, C.N., DelProposto, J.B., Westcott, D.J., and Saltiel, A.R. (2008). Phenotypic switching of adipose tissue macrophages with obesity is generated by spatiotemporal differences in macrophage subtypes. Diabetes *57*, 3239–3246.

Luttrell, L.M., Ferguson, S.S., Daaka, Y., Miller, W.E., Maudsley, S., Della Rocca, G.J., Lin, F., Kawakatsu, H., Owada, K., Luttrell, D.K., et al. (1999). Beta-arrestin-dependent formation of beta2 adrenergic receptor-Src protein kinase complexes. Science *283*, 655–661.

Luttrell, L.M., and Lefkowitz, R.J. (2002). The role of beta-arrestins in the termination and transduction of G-protein-coupled receptor signals. J. Cell Sci. *115*, 455–465.

Miller, W.E., and Lefkowitz, R.J. (2001). Expanding roles for beta-arrestins as scaffolds and adapters in GPCR signaling and trafficking. Curr. Opin. Cell Biol. *13*, 139–145.

Neschen, S., Morino, K., Dong, J., Wang-Fischer, Y., Cline, G.W., Romanelli, A.J., Rossbacher, J.C., Moore, I.K., Regittnig, W., Munoz, D.S., et al. (2007). n-3 Fatty acids preserve insulin sensitivity in vivo in a peroxisome proliferator-activated receptor-alpha-dependent manner. Diabetes *56*, 1034–1041.

Nguyen, M.T., Favelyukis, S., Nguyen, A.K., Reichart, D., Scott, P.A., Jenn, A., Liu-Bryan, R., Glass, C.K., Neels, J.G., and Olefsky, J.M. (2007). A subpopulation of macrophages infiltrates hypertrophic adipose tissue and is activated by free fatty acids via Toll-like receptors 2 and 4 and JNK-dependent pathways. J. Biol. Chem. *282*, 35279–35292.

Oh, D.Y., Song, J.A., Moon, J.S., Moon, M.J., Kim, J.I., Kim, K., Kwon, H.B., and Seong, J.Y. (2005). Membrane-proximal region of the carboxyl terminus of the gonadotropin-releasing hormone receptor (GnRHR) confers differential signal transduction between mammalian and nonmammalian GnRHRs. Mol. Endocrinol. *19*, 722–731.

Polozova, A., and Salem, N., Jr. (2007). Role of liver and plasma lipoproteins in selective transport of n-3 fatty acids to tissues: a comparative study of 14C-DHA and 3H-oleic acid tracers. J. Mol. Neurosci. *33*, 56–66.

Schenk, S., Saberi, M., and Olefsky, J.M. (2008). Insulin sensitivity: modulation by nutrients and inflammation. J. Clin. Invest. *118*, 2992–3002.

Schulte, G., and Fredholm, B.B. (2003). Signaling from adenosine receptors to mitogen-activated protein kinases. Cell Signal *15*, 813–827.

Shoelson, S.E., Herrero, L., and Naaz, A. (2007). Obesity, inflammation, and insulin resistance. Gastroenterology *132*, 2169–2180.

Solinas, G., Vilcu, C., Neels, J.G., Bandyopadhyay, G.K., Luo, J.L., Naugler, W., Grivennikov, S., Wynshaw-Boris, A., Scadeng, M., Olefsky, J.M., and Karin, M. (2007). JNK in hematopoietically derived cells contributes to diet-induced inflammation and insulin resistance without affecting obesity. Cell Metab. *6*, 386–397.

Takaesu, G., Surabhi, R.M., Park, K.J., Ninomiya-Tsuji, J., Matsumoto, K., and Gaynor, R.B. (2003). TAK1 is critical for IkappaB kinase-mediated activation of the NF-kappaB pathway. J. Mol. Biol. *326*, 105–115.

Tazoe, H., Otomo, Y., Kaji, I., Tanaka, R., Karaki, S.I., and Kuwahara, A. (2008). Roles of short-chain fatty acids receptors, GPR41 and GPR43 on colonic functions. J. Physiol. Pharmacol. *59* (*Suppl 2*), 251–262.

Ulloa-Aguirre, A., Stanislaus, D., Janovick, J.A., and Conn, P.M. (1999). Structure-activity relationships of G protein-coupled receptors. Arch. Med. Res. *30*, 420–435.

Wang, J., Wu, X., Simonavicius, N., Tian, H., and Ling, L. (2006a). Medium-chain fatty acids as ligands for orphan G protein-coupled receptor GPR84. J. Biol. Chem. *281*, 34457–34464.

Wang, Y., Tang, Y., Teng, L., Wu, Y., Zhao, X., and Pei, G. (2006b). Association of beta-arrestin and TRAF6 negatively regulates Toll-like receptor-interleukin 1 receptor signaling. Nat. Immunol. *7*, 139–147.

Weisberg, S.P., McCann, D., Desai, M., Rosenbaum, M., Leibel, R.L., and Ferrante, A.W., Jr. (2003). Obesity is associated with macrophage accumulation in adipose tissue. J. Clin. Invest. *112*, 1796–1808.

Xiao, K., McClatchy, D.B., Shukla, A.K., Zhao, Y., Chen, M., Shenoy, S.K., Yates, J.R., 3rd, and Lefkowitz, R.J. (2007). Functional specialization of beta-arrestin interactions revealed by proteomic analysis. Proc. Natl. Acad. Sci. USA *104*, 12011–12016.

Xu, H., Barnes, G.T., Yang, Q., Tan, G., Yang, D., Chou, C.J., Sole, J., Nichols, A., Ross, J.S., Tartaglia, L.A., and Chen, H. (2003). Chronic inflammation in fat plays a crucial role in the development of obesity-related insulin resistance. J. Clin. Invest. *112*, 1821–1830.